

## Effect of the Electron Correlational Screening upon the Calculated Transition Energies of Aromatic Hydrocarbons

Koichi HIRANO\*

Department of Chemistry, Miyagi University of Education, Aramaki-aoba, Sendai 980

(Received September 11, 1986)

A new formalism for two-center repulsion  $\Gamma_{\mu\nu}$ , including a correlational screening factor, is presented. As a criterion of the screening strength, a parameter  $\rho$  (defined by Eq. 13) was introduced. Using  $\Gamma_{\mu\nu}$  and  $\rho$ , transition energy calculations were performed for aromatic hydrocarbons based on the P.P.P scheme. Calculated transition energies decreases as  $\rho$  increases. Adjusting  $\rho$ , we can obtain correct values of the transition energies. That optimal  $\rho$  values extend over the region 0.3–0.5 indicates the extent of that electron correlation is intermediate. The screening caused by the Ohono-Klopman and Nishimoto-Mataga formulae is very close to that by  $\Gamma_{\mu\nu}$ 's whose  $\rho$  values are 0.2 and 0.6. A linear relationship was found between  $\rho$  and  $n$ , the number-density of  $\pi$  electrons. Making use of it, a trial calculation of the anthracene transition energies was made and obtained results were quite acceptable.

Electron correlation is very important in many electron systems, such as atoms and molecules.<sup>1)</sup> In this regard, Gutefreund and Little have evaluated the effect of electron correlation upon low-lying  $\pi$ - $\pi^*$  transitions by means of a random-phase approximation (RPA), in the framework of the P.P.P method.<sup>2,3)</sup>

Kitaura and Nishimoto<sup>4)</sup> also studied this problem using a different RPA formalism, derived by Dunning and Mckoy.<sup>5)</sup> Their studies surely improved the calculation of the transition energies for  $\pi$ -conjugated systems.

Here, however, it must be noted that the validity of RPA is restricted to region where the electron density is high, where the inter-electronic spacing is smaller than the Bohr radius. The  $\pi$  electrons in conjugated systems are not so dense in the above sense. Therefore, RPA is rather inappropriate<sup>6–8)</sup> for accurately describing the  $\pi$ -electron correlation. Thus, it is worthwhile studying this problem using another model which satisfies the requirement of the short-range behavior of Coulomb repulsion since at lower densities electron correlation due to short-range repulsion becomes very significant.<sup>9)</sup> For this purpose we employed a Monte-Carlo screening potential model.<sup>10,11)</sup> The reason for this is that this model satisfies the requirement of a radial distribution function of a two-dimensional classical electron fluid whose density is considerably low.<sup>12)</sup> In the present paper we derived a new formula for a two-center repulsion based upon a Monte-Carlo screening potential model (MCP) while making use of it in transition energy calculations that were performed for aromatic hydrocarbons. In the following, we briefly describe the most important part of the results:

- (1) The new formula for the two-center repulsion.
- (2) The correlational effects upon the MO quantities.
- (3) The number-density dependence of the correlational parameters.

### Model and Method

#### New Formula for Two-Center Repulsion. Accord-

ing to the physics of strong-coupled classical plasmas,<sup>13,14)</sup> let  $H(r)$  be the linear screening potential due to the many-particle correlations (defined by DeWitt et al.);<sup>15)</sup> then the effective potential between two particles,  $V(r)$ , in the liquid phase can be expressed in the form

$$V(r) = \frac{(Ze)^2}{r} - H(r), \quad (1)$$

where  $Ze$  is the electric charge of a particle and  $r$  is the separation between two particles. This potential satisfies the radial distribution function  $g(r)$  of the particles:

$$g(r) = \exp[-V(r)/kT]. \quad (2)$$

By analyzing the results of Monte Carlo studies by Brush et al.,<sup>10)</sup> Itho and Ichimaru<sup>16)</sup> found that apart from the vicinity of  $r=0$ ,  $H(r)$  takes a linear form in the interval  $1.0 \leq r/a \leq 2.0$ :

$$H(r) = \frac{(Ze)^2}{a} \left( c_0 - \frac{c_1 r}{a} \right), \quad (3)$$

where  $a=(3/4 \pi n)^{1/3}$  is the ion-sphere radius and  $n$  the number-density of the particles;  $c_0$  and  $c_1$  satisfy

$$c_1 = \left( \frac{c_0}{2} \right)^2. \quad (4)$$

Here, we notice that by replacing the second term in  $H(r)$  by  $(c_2 r/a)^2$ , we obtain a Salpeter-Horn type screening potential.<sup>14)</sup>

Substituting  $H(r)$  into Eq. 1 and putting  $Z=1$ , we obtain the effective potential  $V(r)$  for two electrons in the liquid phase:

$$V(r) = \frac{e^2}{r} - \frac{e^2}{a} \left( c_0 - \frac{c_1 r}{a} \right), \quad (5)$$

where  $a$  is the Wigner-Seitz sphere radius via  $a=(3/4 \pi n)^{1/3}$  which corresponds to the ion-sphere radius mentioned above. This potential solely holds for two dimensional classical electron liquid.<sup>17)</sup>

In obtaining Eq. 5, we assumed that electrons obey classical statics. In the  $\pi$ -electron case, however, special quantum effects must be taken into account, since

the number-densities of  $\pi$  electrons, (Table 1), are higher than those for a classical electron liquid.<sup>18)</sup> In spite of this, we assume here that  $\pi$  electrons obey classical statics and that Eq. 5 holds for them. This is very crude; however, we accept it as the zeroth-order approximation. The reason for this is as following: Monte Carlo simulations of fermion systems<sup>18)</sup> and analytic calculations on the correlational properties of the degenerate electron fluid have been hitherto made;<sup>19)</sup> however, a formalism which can be applied to the  $\pi$ -electron systems has yet not been established. As a consequence, we derived a  $\pi$ -electron two-center repulsion  $\Gamma_{\mu\nu}$  from Eq. 5, using a point-charge approximation:<sup>20)</sup>

$$\Gamma_{\mu\nu} = \frac{e^2}{R_{\mu\nu}} - \frac{e^2}{d} \left( C_0 - \frac{C_1 R_{\mu\nu}}{d} \right), \quad R_{\mu\nu} < \frac{C_0}{C_1} d$$

and

$$= \frac{e^2}{R_{\mu\nu}}, \quad R_{\mu\nu} > \frac{C_0}{C_1} d,$$

where  $R_{\mu\nu}$  is the internuclear separations,  $d$  is the length parameter and  $C_0$  and  $C_1$  are dimensionless constants. Hereafter, we call  $\Gamma_{\mu\nu}$  the MCP two-center repulsion; it corresponds to  $\gamma_{\mu\nu}$  of the P.P.P scheme.

Next, we consider the physical significance of the new formula  $\Gamma_{\mu\nu}$ . A qualitatively good description is that  $\Gamma_{\mu\nu}$  implies electrostatic interactions due to a potential felt at the center of the Wigner-Seitz sphere of the electrons at the  $\mu$  core from an electron on the  $\nu$ -th core as well as its surrounding polarization field. It arises from a charge depletion in the vicinity of the electron by correlation. This interpretation is based on the ion-sphere model provided for the explanation of short-range screening in a strongly coupled classical plasma.<sup>13,14)</sup>

**Characteristics of  $\Gamma_{\mu\nu}$ .** In this section, we describe a suitable parameter choice and the  $R_{\mu\nu}$ -dependence of  $\Gamma_{\mu\nu}$ . As an example, we show the pyrene case. The length parameter was evaluated as  $d=1.57 \text{ \AA}$ , based upon two distinct roots: Wigner-Seitz sphere radius  $a=1.57 \text{ \AA}$  and radius of Coulomb hole,<sup>21,22)</sup>  $r_{\text{Ch}}=1.1 \text{ \AA}$ . The dimensionless parameters by which correlational screening is characterized were determined as  $C_0=0.95$  and  $C_1=0.50$ , respectively, by means of a trial- and-error method.

A set of parameters, thus determined, yield

$$\Gamma_{\mu\nu} = \frac{14.398}{R_{\mu\nu}} + 4.607 R_{\mu\nu} - 10.942 \text{ eV for } R_{\mu\nu} < 2.37 \text{ \AA},$$

and

$$= \frac{14.398}{R_{\mu\nu}} \text{ eV for } R_{\mu\nu} \geq 2.37 \text{ \AA}.$$

Making use of Eq. 7, we can calculate pyrene transition energies which are in fairly good agreement with the experimental spectra.

Then, we describe the characteristic feature of  $\Gamma_{\mu\nu}$ . In Fig. 1, we display the  $R_{\mu\nu}$ -dependence of in compari-

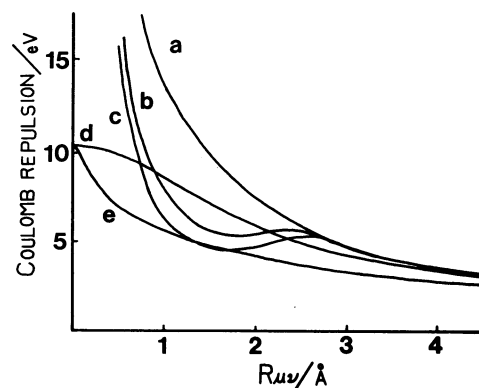


Fig. 1. Comparison of the different forms of effective Coulomb-repulsion:

a): Bare Coulomb potential, b): MCP potential,  $C_1=0.50$ , c): MCP potential,  $C_1=0.45$ , d): Ohono-Klopman potential, e): Nishimoto-Mataga potential.

son with those of Ohono-Klopman,<sup>23,24)</sup>  $\gamma^{\text{OK}}$ , (OK) and Nishimoto-Mataga,<sup>25)</sup>  $\gamma^{\text{NM}}$  (NM) expressions and of the bare Coulomb repulsion:

$$\gamma^{\text{OK}}_{\mu\nu} = \frac{e^2}{\sqrt{a_{\mu\nu}^2 + R_{\mu\nu}^2}}, \quad (8)$$

and

$$\gamma^{\text{NM}}_{\mu\nu} = \frac{e^2}{a_{\mu\nu} + R_{\mu\nu}}, \quad (9)$$

with

$$\frac{1}{a_{\mu\nu}} = \frac{1}{2} \left( \frac{\gamma_{\mu\mu}}{14.398} + \frac{\gamma_{\nu\nu}}{14.398} \right), \quad (10)$$

where  $\gamma_{\mu\mu}$  and  $\gamma_{\nu\nu}$  denote a one-center repulsion at cores  $\mu$  and  $\nu$ . For C-C bonds, we take  $a_{\mu\nu}=1.358 \text{ \AA}$ .

As Fig. 1 shows, the most striking features of our model potential are: (1)  $\Gamma_{\mu\nu}$  has a local minimum at a small distance,  $R_{\mu\nu} \approx 1.5 \text{ \AA}$ ; hence,  $\Gamma_{12} < \Gamma_{13}$ . This result, however, is not so surprising. Since a quite similar result can be seen for the Salpeter-Horn potential<sup>14)</sup> for the strong-screening regime. Moreover, a similar structure can also be found in the Jastrow pseudopotential curves of a Lenard-Jones Bose fluid.<sup>26)</sup> (2) The rapid decrement of  $\Gamma_{\mu\nu}$  at small distances implies a reduction of the bare Coulomb repulsion due to correlational screening; the strength of the screening is strongly parameter sensitive. Therefore, one of the reasons that  $\Gamma_{12} < \Gamma_{13}$  may be ascribable to the choice of parameter. (3) By a suitable parameter choice,  $\Gamma_{\mu\nu}$  can be determined so as to give the correct values of the MO quantities.

Based on the above, we can perform MO calculations that take the electron-correlation effect into account by using  $\Gamma_{\mu\nu}$ . This is because, in the study, we employed  $\Gamma_{\mu\nu}$  as a two-center repulsion. Hence, the following equality still holds:

$$\gamma_{\mu\nu} = \Gamma_{\mu\nu}. \quad (11)$$

Table 1. Parameters for Aromatic Hydrocarbons

	Benzene	Naphthalene	Anthracene	Pyrene	Coronene
$n \text{ cm}^{-3\text{a}}$	$4.0 \times 10^{22}$	$5.4 \times 10^{22}$	$5.9 \times 10^{22}$	$6.1 \times 10^{22}$	$6.6 \times 10^{22}$
$a \text{ \AA}^{\text{b}}$	1.69	1.64	1.59	1.58	1.53
$d \text{ \AA}^{\text{c}}$	1.25	1.25	1.25	1.25	1.25
$C_0$	0.95	0.95	0.95	0.95	0.95
$C_1$	0.61	0.53	0.50 <sup>d</sup>	0.50	0.47
$\rho$	0.30	0.40	0.43 <sup>e</sup>	0.43	0.48

a) Number-density of  $\pi$  electrons. b) Radius of Wigner-Seitz sphere. c) Length parameter. d) Estimated from Eq. 14. e) Estimated from Eq. 18.

**MO Calculation.** P.P.P.-Type SCF-MO calculations were made. In the actual calculations, singly excited configurations higher than 8–10 eV were taken into account. All of the C–C bond lengths and the bond angles were set to 1.39 Å and 120°, respectively. The one-center core integral and the one-center repulsion were evaluated from the valence state ionization potentials and the electron affinities viz.  $W_{\mu\mu}=11.22$  and  $\gamma_{\mu\mu}=10.60$  eV.<sup>27)</sup> A two-center core integral was evaluated by the Wolfsberg-Helmholtz's formula with  $K=0.96$ .<sup>28)</sup>

$$\beta_{\mu\nu} = \frac{K}{2} S_{\mu\nu} (W_{\mu\mu} + W_{\nu\nu}), \quad (12)$$

where  $S_{\mu\nu}$  is the overlap integral between cores  $\mu$  and  $\nu$ .

For simplicity, we consider that  $C_1$  alone is variant and that the other parameters are invariant. Then, in the present calculations, we varied  $\Gamma_{\mu\nu}$  by changing  $C_1$ . In Table 1 the parameters used are listed with other related quantities.

## Results and Discussion

**Degrees of Screening.** As a criterion of electron correlation, we introduced here a new parameter  $\rho$ , degrees of screening:

$$\rho = 1 - \frac{\Gamma_0}{U_0}, \quad (13)$$

where  $\Gamma_0$  and  $U_0$  are, respectively, the two-center and the bare Coulomb repulsion at the nearest-neighbor distance. It is obvious from the equation that when  $\Gamma_0=U_0$ ,  $\rho=0$ , (without screening) and if  $\Gamma_0=0$ ,  $\rho=1$ , (full screening). For intermediate screening,  $\rho$  satisfies  $0 < \rho < 1$ .

As a consequence, we can express the relative strength of the electron correlation in terms of  $\rho$ . Then, we study the effect of the electron correlation on the transition energies using  $\rho$ . For this purpose we derived a parametric formula (14) utilizing Eq. 13 and 6 (where we take a nearest-neighbor distance  $R_0=1.39$  Å):

$$C_1 = 0.854 - 0.809\rho. \quad (14)$$

Making use of this relationship, we can determine a suitable  $\Gamma_{\mu\nu}$  for setting the  $\rho$  values. This makes it possible to calculate the MO quantities as a function of  $\rho$ . Analysing the  $\rho$ -dependence of the calculated quantities, we can evaluate the electron correlation

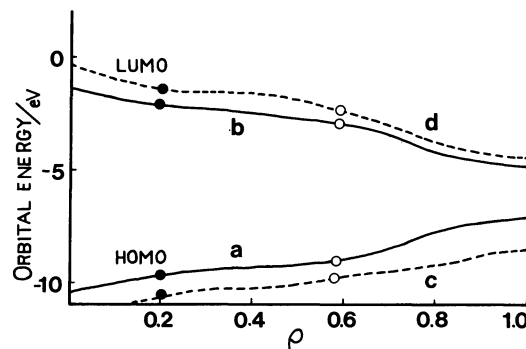


Fig. 2.  $\rho$ -Dependence of the orbital energy. —: Pyrene, a)  $E_H$ , b)  $E_L$ , ----: Naphthalene, c)  $E_H$ , d)  $E_L$ , ●: Ohono-Klopman, ○: Nishimoto-Mataga.

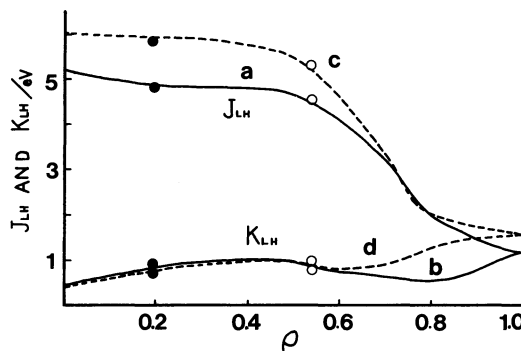


Fig. 3.  $\rho$ -Dependence of Coulomb and exchange repulsion. —: Pyrene, a)  $J_{LH}$ , b)  $K_{LH}$ , ----: Naphthalene, c)  $J_{LH}$ , d)  $K_{LH}$ , ●: Ohono-Klopman, ○: Nishimoto-Mataga.

effect upon the quantities.

**$\rho$ -Dependence of Transition Energies.** Here we describe the naphthalene and pyrene cases. Figures 2, 3 show the  $\rho$ -dependence of the orbital energies as well as the Coulomb and exchange repulsion.

Figure 4 shows the  $\rho$ -dependence of the calculated transition energies. As was seen in Fig. 2, the HOMO-levels,  $E_H$ 's, increase with increasing  $\rho$  and the LUMO-levels,  $E_L$ 's, are lower as  $\rho$  increases. As a result, the orbital spacing becomes narrow with increasing  $\rho$ . This can be explained according to the following interpretation by Hush and Pople.<sup>29)</sup> Let  $\Delta E_{LH}$  be the orbital spacing between LUMO and HOMO; then

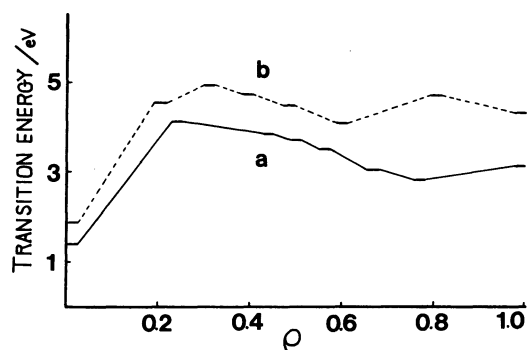


Fig. 4.  $\rho$ -Dependence of the transition energies. a): Pyrene lowest  $B_{2u}$ , b): Naphthalene lowest  $B_{2u}$ .

$$\Delta E_{LH} = E_L - E_H$$

$$= 2 \sum_{\mu < \nu}^{\text{bond}} \beta_{\mu\nu} (C_{L\mu} C_{L\nu} - C_{H\mu} C_{H\nu}) - \sum_{\mu < \nu} P_{\mu\nu} (C_{L\mu} C_{L\nu} - C_{H\mu} C_{H\nu}) \Gamma_{\mu\nu}. \quad (15)$$

Here,  $E_L$  and  $E_H$  are the orbital energies of LUMO and HOMO;  $C_{L\mu}$ ,  $C_{H\nu}$ , and  $P_{\mu\nu}$  are the AO coefficients and the  $\pi$ -bond order between cores  $\mu$  and  $\nu$ . To derive the above equation, we used the following approximation:

$$F_{\mu\nu} = \beta_{\mu\nu} - \frac{1}{2} P_{\mu\nu} \Gamma_{\mu\nu}, \quad (16)$$

where  $F_{\mu\nu}$  is the off-diagonal elements of the  $F$ -matrix<sup>30)</sup> and  $\beta_{\mu\nu}=0$  for non-neighbor  $\mu$  and  $\nu$ .

The above equation shows that  $\Delta E_{LH}$  is reduced when  $\Gamma_{\mu\nu}$  decrease; namely,  $\rho$  increases since  $\Gamma_{\mu\nu}$  is inversely related to  $\rho$  and the second summation takes a positive value. This is because, the orbital spacing becomes narrow as  $\rho$  increases (Fig. 2). Next, we describe the  $\rho$ -dependence of the transition energies. As Fig. 4 shows, for intermediate  $\rho$  values (i.e.,  $0.2 < \rho < 0.6$ ) the transition energies decrease as  $\rho$  increases. Judging from the  $\rho$ -dependence of the  $\Delta E_{LH}$ 's, this is fairly acceptable. Out of the regions, however, the  $\Delta E$ 's exhibit somewhat irregular changes. This abnormality is probably due to the characteristic  $\rho$ -dependence of the Coulomb and exchange repulsion,  $J_{LH}$  and  $K_{LH}$ , because these quantities are correlated with  $\Delta E$  through the following formalism:<sup>31)</sup>

$$\Delta E = \Delta E_{LH} - J_{LH} + 2K_{LH}. \quad (17)$$

To explain the  $\Delta E$  vs.  $\rho$  curves more exactly, however, the  $\rho$ -dependence of the CI matrix elements must be taken into account, since changes in the CI matrix elements strongly alter the transition energies, even if the changes are not so remarkable. This problem will be reported elsewhere.

Here, we direct our attention to a comparison of the new formula  $\Gamma_{\mu\nu}$  to that of OK and NM. For this purpose, the calculated results by  $\gamma_{\mu\nu}^{OK}$  and  $\gamma_{\mu\nu}^{NM}$  are also plotted in Figs. 2, 3. As can be seen from the figures, the values calculated by using OK and NM are in fairly

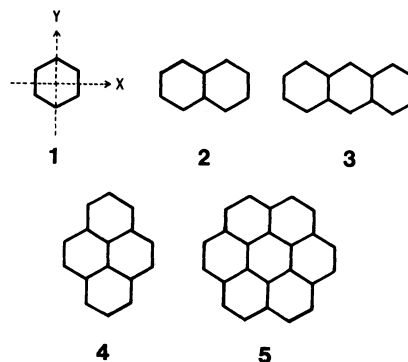


Fig. 5. Coordinate systems and carbon skeletons of the molecules. 1) Benzene, 2) Naphthalene, 3) Anthracene, 4) Pyrene, 5) Coronene.

good agreement with those by using  $\Gamma_{\mu\nu}$ 's (whose values are about 0.2 and 0.6, respectively).

This indicates that the relative values of correlational screening estimated from OK and NM are in the ratio of 1/3. With regard to this, a very similar result has been reported by Fukutome and Sasai<sup>32)</sup> while studying the electron correlation in linear polyenes. Their proposal can be summarized as follows: The value of  $(\gamma_{\mu\mu} - \gamma_0)/|\beta|$  that determines the extent of electron correlation, is about 1 for OK and about 3 for NM. Here,  $\gamma_{\mu\mu}$  is the one-center repulsion and  $\gamma_0$  the nearest-neighbor two-center repulsion.  $\beta$  is the nearest-neighbor two-center core integral. These facts imply that OK is acceptable when the electron correlation is weak, whereas NM is good when the correlation is rather strong.

**Transition Energies.** Here, we described the transition energies calculated using  $\Gamma_{\mu\nu}$ . The coordinate systems<sup>33)</sup> and carbon skeletons of the molecules are illustrated in Fig. 5. In Tables 2—5 the transition energies, oscillator strength and order of states are given in comparison with other calculated and experimental data. From the tables we can see that MCP gives fairly good results (as compared with the other calculations). In the case of MCP, the optimal  $\rho$  values are shown in parentheses, where the  $\rho$  values extend over the region 0.3—0.5. This indicates that the degrees of correlation in these molecules is intermediate.

Moreover, a striking feature found in the above tables is that the energy-level spacings and order of states calculated by the MCP are rather close to those by the  $\beta$ -variable method.<sup>39,40)</sup> This is probably due to a procedural similarity between the two methods, since for both MCP and  $\beta$ -variable, the off-diagonal elements of  $F$ -matrix are corrected so as to reproduce the experimental spectra by changing the adjustable parameters of  $C_1$  and  $\beta_0$ .

Next, we describe the number-density dependence of  $\rho$ . As can be clearly seen in Table 1, when the molecular size becomes large,  $\rho$  increases in parallel with  $n$ . This feature suggests that some definite relationship

Table 2. Transition Energies and Intensities of Benzene

State	NM		RPA <sup>34)</sup>		MCP ( $\rho=0.30$ )		Obsd <sup>35)</sup>	
	$\Delta E/\text{eV}$	$f$	$\Delta E/\text{eV}$	$f$	$\Delta E/\text{eV}$	$f$	$\Delta E/\text{eV}$	$f$
$B_{2u}$	5.48	0.00	4.86	0.00	5.27	0.00	4.71	0.002
$B_{1u}$	6.66	0.00	4.77	0.00	6.49	0.00	5.96	0.10
$E_{1u}$	7.48	1.26	6.99	1.537	7.00	1.18	6.76	0.69

Table 3. Transition Energies and Intensities of Naphthalene

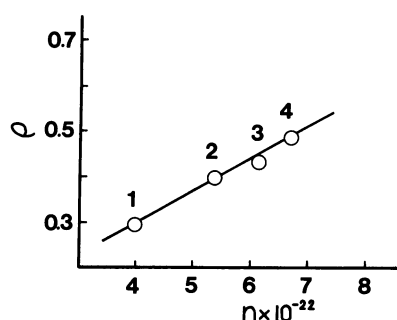
State	NM		$\beta$ -variable <sup>36)</sup>		MCP ( $\rho=0.40$ )		Obsd <sup>35)</sup>	
	$\Delta E/\text{eV}$	$f$	$\Delta E/\text{eV}$	$f$	$\Delta E/\text{eV}$	$f$	$\Delta E/\text{eV}$	$f$
$B_{3u}$	4.62	0.00	3.98	0.00	4.42	0.00	3.97	0.002
$B_{2u}$	4.77	0.297	4.51	0.246	4.75	0.51	4.29	0.18
$B_{3u}$	6.22	2.22	5.54	1.946	5.99	2.05	5.64	1.70
$B_{2u}$	6.93	0.651	6.07	0.861	6.70	0.65	6.53	0.20

Table 4. Transition Energies and Intensities of Pyrene

State	NM		$\beta$ -variable <sup>36)</sup>		MCP ( $\rho=0.43$ )		Obsd <sup>37, 38)</sup>	
	$\Delta E/\text{eV}$	$f$	$\Delta E/\text{eV}$	$f$	$\Delta E/\text{eV}$	$f$	$\Delta E/\text{eV}$	$f$
$B_{3u}$	—	—	3.49	0.00	3.79	0.00	3.33	0.002
$B_{2u}$	3.80	0.972	3.64	0.675	3.81	0.89	3.71	0.33
$B_{3u}$	5.28	1.17	4.77	0.954	4.98	1.06	4.55	0.35
$B_{2u}$	6.14	1.59	5.25	1.48	5.86	1.58	5.14	0.85

Table 5. Transition Energies and Intensities of Coronene

State	NM		$\beta$ -variable <sup>36)</sup>		MCP ( $\rho=0.48$ )		Obsd <sup>37, 38)</sup>	
	$\Delta E/\text{eV}$	$f$	$\Delta E/\text{eV}$	$f$	$\Delta E/\text{eV}$	$f$	$\Delta E/\text{eV}$	$f$
$B_{2u}$	3.43	0.00	3.04	0.00	3.39	0.00	2.91	0.0
$B_{1u}$	3.83	0.00	3.51	0.00	4.01	0.001	3.66	0.10
$E_{1u}$	4.67	5.86	4.19	3.89	4.49	3.90	4.18	1.34

Fig. 6. Relation between  $\rho$  and  $n$ :  $\rho$  is the degrees of screening and  $n$  the number-density of  $\pi$  electrons.

exists between them. In fact, plots of  $\rho$  against  $n$  show the following relationship (displayed in Fig. 6):

$$\rho = 7.00n \times 10^{-24} + 0.02, \quad (18)$$

with

$$n = \frac{\nu DN}{M}. \quad (19)$$

Here,  $\nu$  is the number of  $\pi$  electrons,  $D$  the density of the materials,  $N$  Avogadro's number and  $M$  the molecular weight. Equation 18 is an empirical formula; therefore, we can not undertake a further analysis. In spite of this, it does a very useful way to perform practical calculations since, by making use of the equation, we can evaluate  $\rho$  for an aromatic hydrocarbon when  $n$  is given.

For checking the validity of the above relationship, a trial calculation was made for anthracene. In the calculation, we took  $\rho=0.34$  (same as putting  $n=5.9 \times 10^{22}$ ). As Table 6 shows, the obtained results are in acceptable agreement with those reported by other authors, except for the appearance of a weak band located above the lowest  $B_{2u}$  band. Generally speaking, this band is closely related to the strength of a two-center repulsion  $\gamma_{\mu\nu}$ . This band appears when  $\gamma_{\mu\nu}$  has a simple Coulomb-like form, as a Slater AO-type repulsion.<sup>41)</sup> Contrariwise, the band disappeared when  $\gamma_{\mu\nu}$  assumed such long-range screened forms as OK,<sup>36)</sup> NM<sup>42)</sup> and a cusp-like shape interaction.<sup>43)</sup> In  $\Gamma_{\mu\nu}$  case, screening is restricted within the interval  $R_{\mu\nu} < C_0 d / C_1$ ; when  $R_{\mu\nu}$  increases beyond this boundary, it

Table 6. Transition Energies and Intensities of Anthracene

State	NM <sup>42)</sup>		$\beta$ -variable <sup>36)</sup>		Rudenberg <sup>43)</sup>		Pariser <sup>41)</sup>		MCP		Obsd <sup>35)</sup>	
	$\Delta E/\text{eV}$	$f$	$\Delta E/\text{eV}$	$f$	$\Delta E/\text{eV}$	$f$	$\Delta E/\text{eV}$	$f$	$\Delta E/\text{eV}$	$f$	$\Delta E/\text{eV}$	$f$
$B_{3u}$	3.989	0.00	3.58	0.00	3.22	0.014	3.715	0.00	4.01	0.00	—	—
$B_{2u}$	3.279	0.26	3.59	0.313	3.59	0.27	3.645	0.386	3.55	0.329	3.34	0.1
							5.251	0.091	5.11	0.177		
$B_{3u}$	5.098	2.74	4.84	2.527	5.26	3.09	5.499	3.229	5.30	2.909	4.84	2.28
$B_{2u}$	6.648	1.03	5.87	0.604	5.47	0.83	6.686	0.640	6.70	0.903	5.61	0.28

results in a Coulomb-like repulsion (Eq. 6). This indicates that the long-range behavior of  $\Gamma_{\mu\nu}$  is very similar to that of a Slater AO-type repulsion when  $R_{\mu\nu}$  becomes large. This is because MCP calculates the weak second lowest  $B_{2u}$  band.

From the above results, we then concluded that MCP provides a semiempirical method that is favorable for studying the electron-correlation effect upon a calculation of the transition energies, (and for which Eq. 17 is available). In order to apply this method more extensively, however, the physical concept of the linear screening potential  $H(r)$  must be clarified based upon a theoretical consideration.

We wish to express our thanks to Prof. Setsuo Ichimaru of University of Tokyo and Dr. Hiroshi Yasuhara of Tohoku University for sending reprints of their work. We thank Dr. Takeshi Ikeyama of Miyagi University of Education for his helpful discussions. We also thank the Computer Center, Tohoku University, for the use of the ACOS 1000 computer.

## References

- 1) S. Wilson, "Electron Correlation in Molecule," Oxford University Press (1984), p. 43.
- 2) H. Gutefreund and W. A. Little, *J. Chem. Phys.*, **50**, 4468 (1969).
- 3) H. Gutefreund and W. A. Little, *Phys. Rev.*, **83**, 68 (1969).
- 4) K. Kitaura and K. Nishimoto, *Theoret. chim. Acta (Berl.)*, **28**, 111 (1973).
- 5) H. T. Dunning and V. Mckoy, *J. Chem. Phys.*, **47**, 1735 (1967).
- 6) D. J. Rowe, *Rev. Mod. Phys.*, **40**, 153 (1968).
- 7) H. Yasuhara and M. Watanabe, *Phys. Soc. Jpn.*, **33**, 576 (1978).
- 8) K. Utsumi and S. Ichimaru, *Phys. Soc. Jpn.*, **36**, 504 (1981).
- 9) H. Yasuhara, *J. Phys. Soc. Jpn.*, **36**, 361 (1974).
- 10) S. G. Brush, H. L. Sahlin, and E. Teller, *J. Chem. Phys.*, **45**, 2101 (1966).
- 11) H. Totsuji, *Phys. Rev. A*, **17**, 399 (1978).
- 12) S. Ichimaru, *Phys. Soc. Jpn.*, **34**, 753 (1979).
- 13) S. Ichimaru, *Rev. Mod. Phys.*, **54**, 1017 (1982).
- 14) E. E. Salpeter and H. M. Van Horn, *Astrophys. J.*, **155**, 183 (1969).
- 15) H. E. DeWitt, H. C. Graboske, and M. S. Cooper, *Astrophys. J.*, **181**, 143 (1973).
- 16) N. Itoh and S. Ichimaru, *Phys. Rev. A*, **16**, 2178 (1977).
- 17) N. Itoh, S. Ichimaru, and S. Nagano, *Phys. Rev. B*, **17**, 2862 (1978).
- 18) M. Imada and M. Takahashi, *J. Phys. Soc. Jpn.*, **53**, 3770 (1984).
- 19) S. Tanaka and S. Ichimaru, *J. Phys. Soc. Jpn.*, **55**, 2278 (1986).
- 20) J. A. Pople, *Trans. Faraday Soc.*, **49**, 1357 (1953).
- 21) B. M. Gimarc, W. A. Coone, and R. G. Parr, *J. Chem. Phys.*, **42**, 21 (1965).
- 22) C. A. Coulson and A. H. Neilson, *Proc. Phys. Soc.*, **78**, 831 (1961).
- 23) K. Ohono, *Theoret. chim. Acta*, **2**, 219 (1964).
- 24) G. Klopman, *J. Am. Chem. Soc.*, **86**, 4550 (1964).
- 25) K. Nishimoto, and N. Mataga, *Z. Phys. Chem. (N. F.)*, **12**, 335 (1957).
- 26) G. Gaglione, G. L. Masserini, and L. Reatto, *Phys. Rev. B*, **22**, 1237 (1980).
- 27) K. Hirano, *Bull. Chem. Soc. Jpn.*, **56**, 850 (1983).
- 28) M. Wolfsberg and L. Helmholz, *J. Chem. Phys.*, **20**, 837 (1952).
- 29) N. S. Hush and J. A. Pople, *Trans. Faraday Soc.*, **51**, 600 (1955).
- 30) C. C. J. Roothaan, *Rev. Mod. Phys.*, **23**, 69 (1951).
- 31) R. G. Parr and R. S. Mulliken, *J. Chem. Phys.*, **18**, 1338 (1950).
- 32) H. Fukutome and M. Sasai, *Prog. Theor. Phys.*, **48**, 41 (1982).
- 33) N. S. Ham and K. Rudenberg, *J. Chem. Phys.*, **25**, 13 (1956).
- 34) K. Kitaura and K. Nishimoto, *Theoret. chim. Acta (Berl.)*, **31**, 91 (1973).
- 35) H. B. Klevens and J. R. Platt, *J. Chem. Phys.*, **17**, 470 (1949).
- 36) K. Nishimoto, *Theoret. chim. Acta (Berl.)*, **7**, 207 (1967).
- 37) J. Tanaka, *Bull. Chem. Soc. Jpn.*, **38**, 86 (1965).
- 38) H. Zimmerman and N. Joop, *Zeit. für Electrochem.*, **65**, 138 (1961).
- 39) K. Nishimoto and L.S. Foster, *Theoret. chim. Acta*, **3**, 407 (1965).
- 40) K. Tomono and K. Nishimoto, *Bull. Chem. Soc. Jpn.*, **49**, 1179 (1976).
- 41) R. Pariser, *J. Chem. Phys.*, **24**, 250 (1956).
- 42) N. Mataga, K. Nishimoto, and S. Mataga, *Bull. Chem. Soc. Jpn.*, **32**, 395 (1959).
- 43) N. S. Ham and K. Rudenberg, *J. Chem. Phys.*, **25**, 1 (1956).